

Supporting Information

In situ Preparation of Catalyst Surface for High Resolution Environmental Transmission Electron Microscopy

Vladimir Roddatis*, **Gaurav Lole**, and **Christian Jooss****

Institute of Materials Physics, University of Goettingen, D-37077, Goettingen, Germany;

* Correspondence: vroddatis@ump.gwdg.de; Tel.: +49-551-39-25026 (V.R.);

** Correspondence: cjooss@gwdg.de; Tel.: +49-551-39-25303 (C.J.);

Received: date; Accepted: date; Published: date

Supporting Figures

Figure S1 - The PCMO ($x=0.33$) after electron beam treatment in He at 50 μ bars.

Figure S2 - The PCMO ($x=0.33$) after electron beam treatment in O₂ at 50 μ bars.

Figure S3 - HRTEM image and rotationally averaged profiles of PCMO in O₂ and in He ($x=0.33$).

Figure S4 - HRTEM image and rotationally averaged profiles of PCMO in He ($x=0.33$).

Figure S5- Analysis of broadening of spots in FFTs, lattice disorder in PCMO ($x=0.1$)

Figure S6-1. Through focus series of HRTEM images of PCMO ($x=0.33$) for the thickness of 10 nm.

Figure S6-2. Experimental and calculated HRTEM images of PCMO ($x=0.33$) for the thickness of 3 nm.

Figure S7 - The PCMO ($x=0.1$) after electron beam treatment in He at 50 μ bars.

Figure S8 - HRSTEM image and EELS spectrum of PrO_x particle at the surface of PCMO ($x=0.33$).

Figure S9 - An example of multiple ion detection scan in Quadera™ software.

Supporting Tables

Table S1. Summary of the Mn valence PCMO ($x=0.33$) after electron beam treatment in He at 50 μ bars.

Table S2. Summary of the Mn valence of PCMO ($x=0.33$) after electron beam treatment in O₂ at 50 μ bars.

Table S3-1. Simulation parameters for the through focus series.

Table S3-2. Simulation parameters for individual experimental images.

Table S4. Summary of the Mn valence of PCMO ($x=0.1$) after electron beam treatment in He at 50 μ bars.

The PCMO ($x=0.33$) after electron beam treatment in He at 50 μ bars.

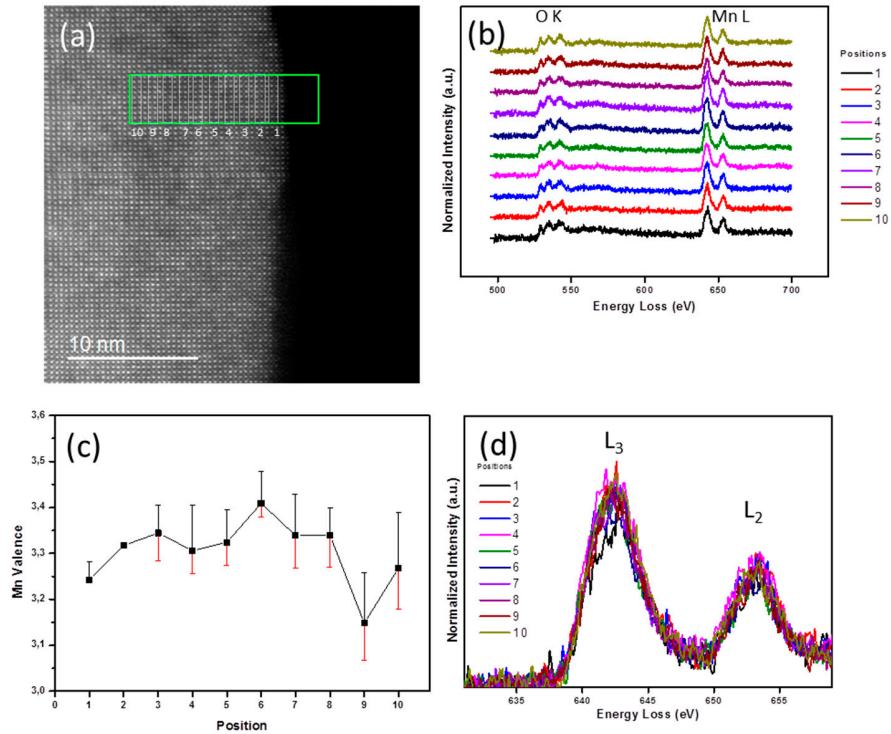


Figure S1. The PCMO ($x=0.33$) after electron beam treatment in He at 50 μ bars. (a) HAADF image; (b) EELS spectra; (c) Mn valence plot; (d) $L_{2,3}$ -edge of Mn at each point.

Table S1. Summary of the Mn valence PCMO ($x=0.33$) after electron beam treatment in He at 50 μ bars.

The average value is 3.30 ± 0.06 .

Position	1	2	3	4	5	6	7	8	9	10
Mn valence	3.24	3.31	3.34	3.31	3.32	3.41	3.34	3.34	3.15	3.27
Error (-)	0	0	-0.06	-0.05	-0.05	-0.03	-0.07	-0.07	-0.08	-0.09
Error (+)	0.04	0	0.06	0.1	0.07	0.07	0.09	0.06	0.11	0.12

The PCMO ($x=0.33$) after electron beam treatment in O_2 at 50 μ bars.

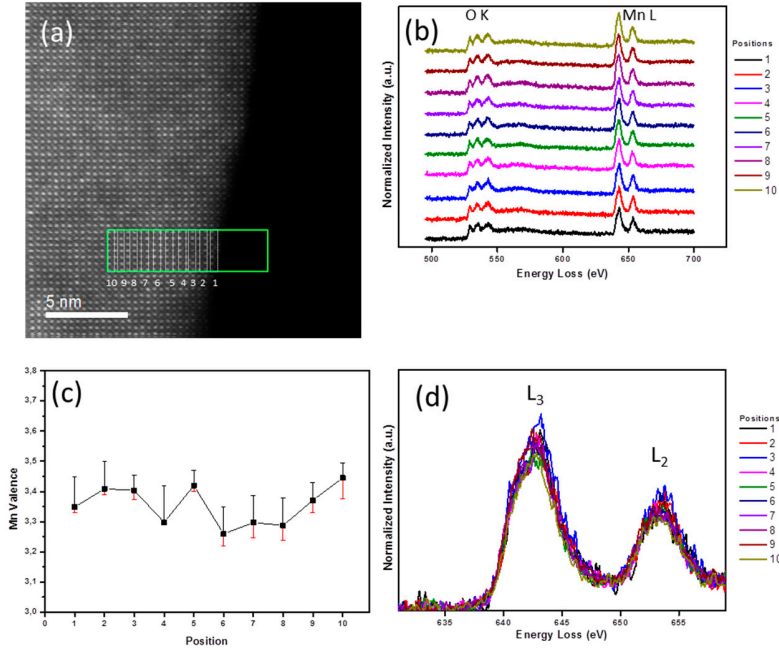


Figure S2. The PCMO ($x=0.33$) after electron beam treatment in O_2 at 50 μ bars. (a) HAADF image; (b) EELS spectra; (c) Mn valence plot; (d) $L_{2,3}$ -edge of Mn at each point.

Table S2. Summary of the Mn valence of PCMO ($x=0.33$) after electron beam treatment in O_2 at 50 μ bars. Average value is 3.36 ± 0.06 .

Position	1	2	3	4	5	6	7	8	9	10
Mn valence	3.35	3.41	3.40	3.30	3.42	3.26	3.30	3.29	3.37	3.45
Error (-)	-0.02	-0.02	-0.03	0.0	-0.02	-0.04	-0.05	-0.05	-0.04	-0.07
Error (+)	0.10	0.09	0.05	0.12	0.05	0.09	0.09	0.09	0.06	0.05

Method of Valence analysis used:

Mn valence state is determined by calculating Mn L_3/L_2 integrated intensity ratio using method demonstrated by M. Varela *et al* (see Ref. 37 in the main text) for $La_xCa_{1-x}MnO_3$ yielding a valence $V = -0.73(11) \times \text{Mn } L_3/L_2 \text{ intensity ratio} + 5.0(4)$. All our EELS spectra are extracted from spectrum images at area of vacuum and at different gas pressure for post-mortem analysis as visible in Figures S1 and 2. A power-law background functions is fit to 50 eV wide windows before each Mn L_3 -edge. A Hartree-Slater (HS) type cross-section step function from Gatan Digital Micrograph is used for correcting the background within the L_3 and L_2 peaks. The HS step function removes continuum contribution by placing a 10 eV window exactly after L_2 edge. The energy axis is calibrated by using the zero loss peak. The error bars are determined by changing the position of integration windows of L_3 and L_2 edges by ± 1 eV. The relative thickness of the lamella region, where the spectra is extracted is $t/\lambda < 0.5$, where $\lambda \approx 50$ nm represents the inelastic scattering length.

Analysis of broadening of spots in FFTs, lattice disorder in PCMO ($x=0.33$)

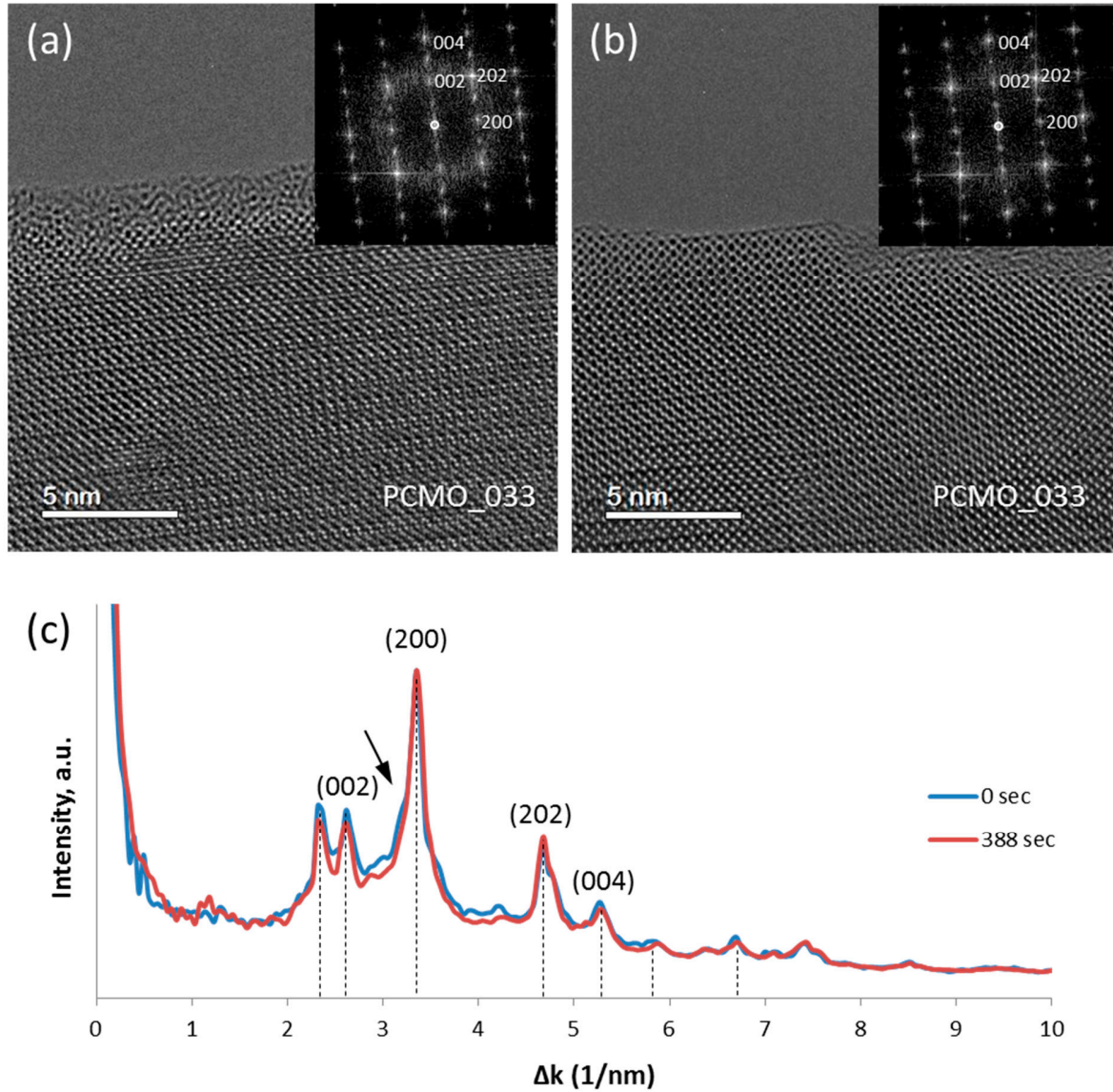


Figure S3. Analysis of broadening of spots in FFTs, lattice disorder in PCMO ($x=0.33$) in O_2 . (a) HRTEM image of PCMO ($x=0.33$) at the beginning and (b) after 388 seconds of electron irradiation in O_2 . (c) The rotationally averaged profiles of corresponding FFTs. The intensities of peaks remain almost unchanged. A shoulder marked with the black arrow originates from the amorphous phase and disappears after 388 seconds.

HRTEM image and rotationally averaged profiles of PCMO in He ($x=0.33$)

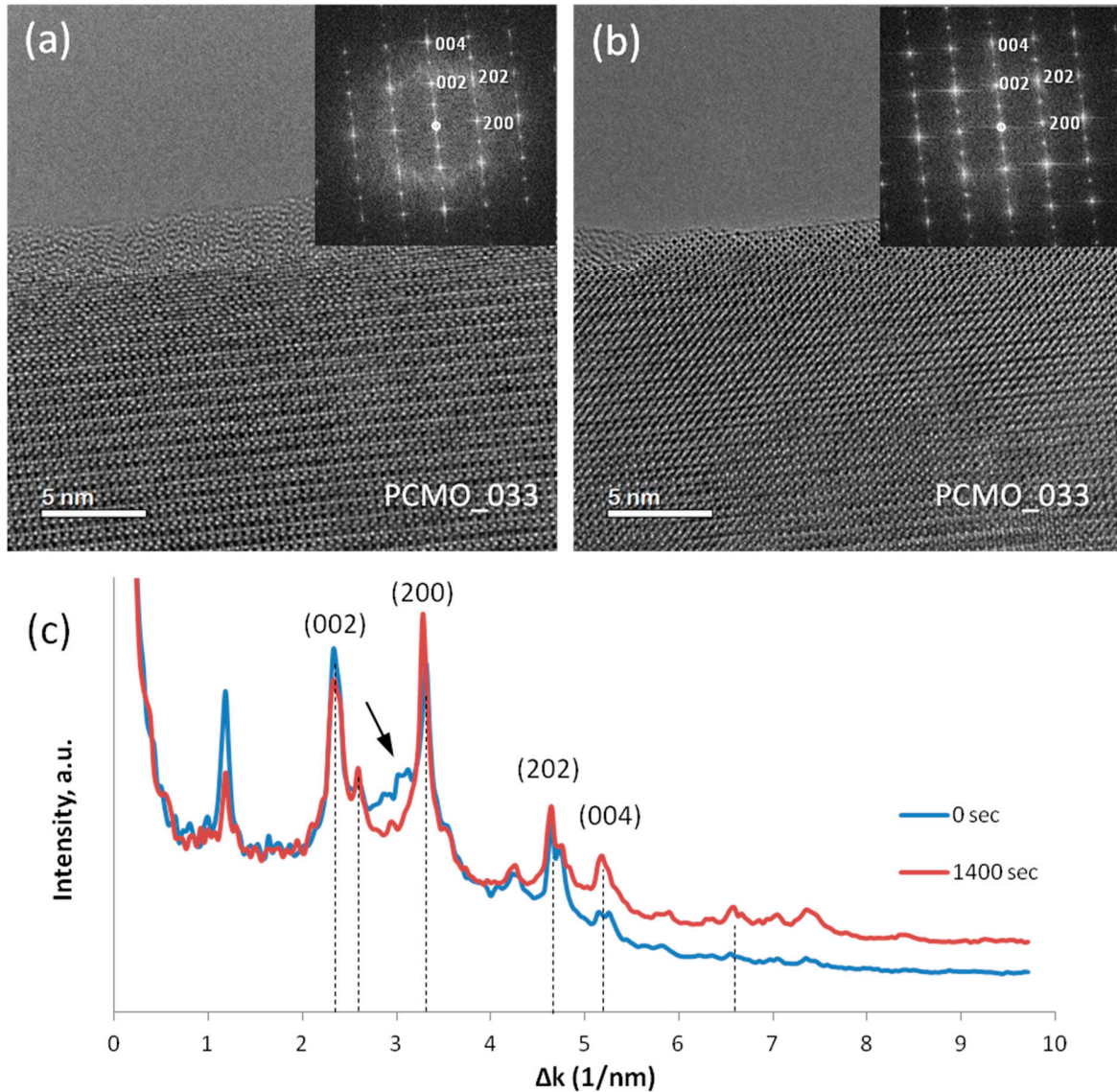


Figure S4. HRTEM image and rotationally averaged profiles of PCMO in He ($x=0.33$). (a) HRTEM image of PCMO ($x=0.33$) at the beginning and (b) after 1400 seconds of electron irradiation in He. (c) The rotationally averaged profiles of corresponding FFTs. The broadening of peaks and change their intensity is visible, revealing the increase of structural disorder. The broad peak marked with the black arrow originates from the amorphous phase and disappears after 1400 seconds.

Analysis of broadening of spots in FFTs, lattice disorder in PCMO ($x=0.1$)

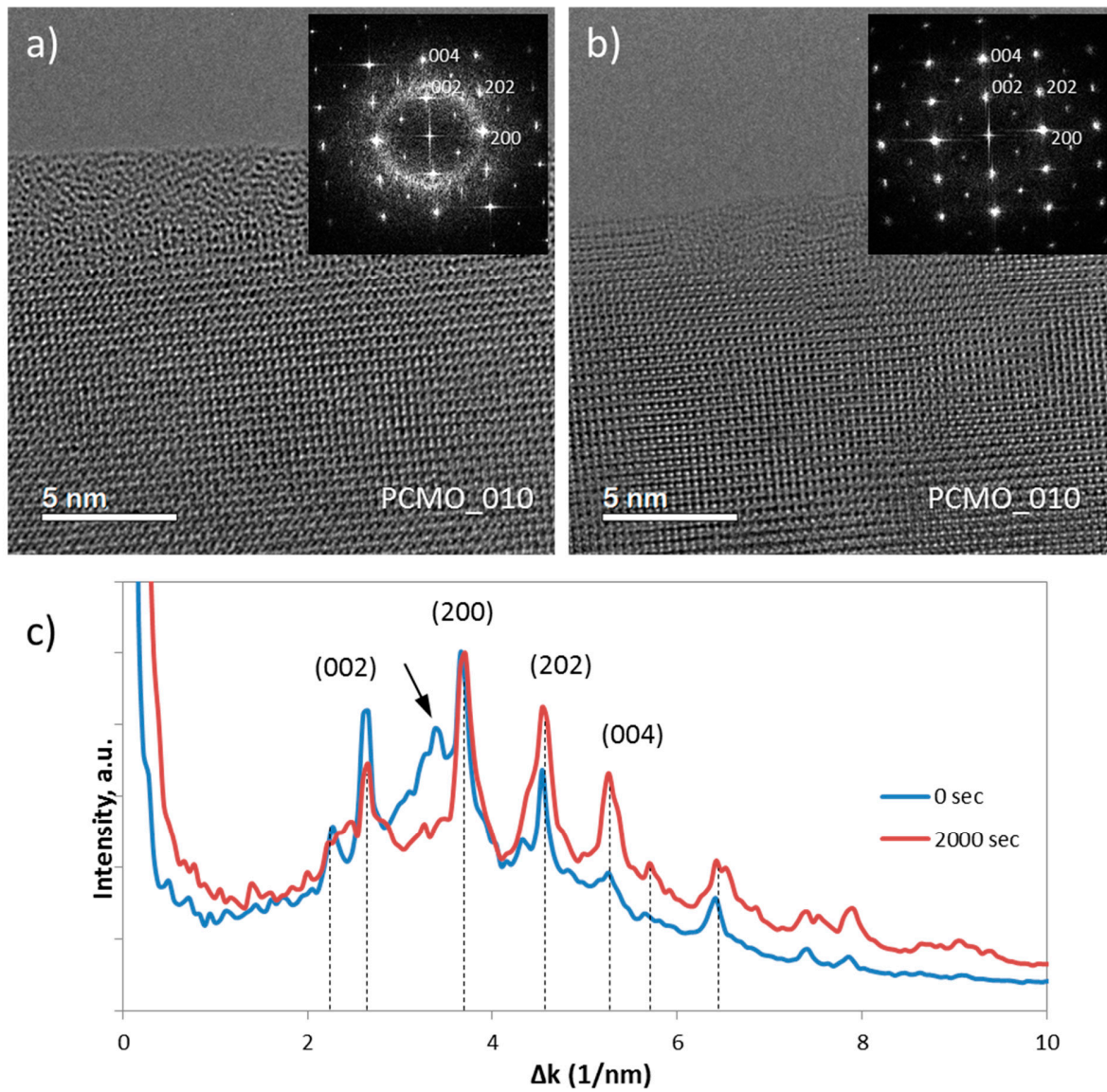


Figure S5. (a) HRTEM image of PCMO ($x=0.1$) at the beginning and (b) after 2000 seconds of electron irradiation. (c) The rotationally averaged profiles of corresponding FFTs. The broadening of peaks and change their intensity is clearly visible, revealing the increase of structural disorder. The broad peak marked with the black arrow originates from the amorphous phase and disappears after 2000 seconds.

HRTEM image simulations and atomic models

Detailed analysis of image conditions in the ETEM was reported by Bugnet et al. (see Ref. [29] in the main text). We followed similar procedure of the microscope tuning to achieve the spherical aberration coefficient (C_s) to a positive value of $10 \pm 5 \mu\text{m}$ when atoms appear in black at the Scherzer defocus. The thickness of edge was estimated from low-loss EELSS spectra yielding a value of less than 10 nm. HRTEM images were calculated using QSTEM software. Parameters of simulations are listed in Table S5-1 and Table S5-2.

Table S3-1: Simulation parameters for the through focus series

Acceleration voltage	300 kV
Defocus C_1	-20 nm - +20 nm
Spherical aberration constant C_3	10 μm
Specimen thickness	10 nm
Emitter energy spread	1 eV

An example of seria of images corresponding to this thickness is shown in the following Figure S5-1. The individual Mn atomic columns are revealed in the narrow interval of defocus values from -12 to -8 nm (marked with the orange frame).

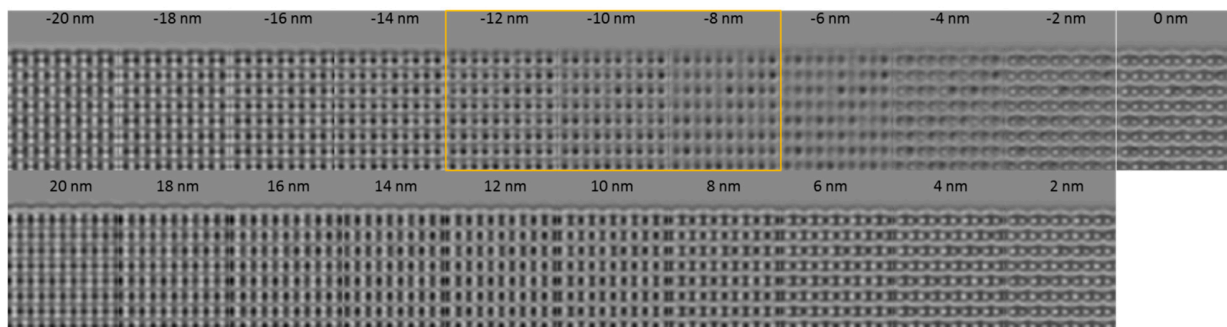


Figure S6-1. Calculated image of B-terminated surface of PCMO ($x=0.33$) projected along [010] corresponding to the thickness of 10 nm

Taking into account the sputtering of material by electron beam the real thickness could be even less than 9 nm. Figure S5-2 shows calculated images of PCMO ($x=0.33$) along [010] and [001] crystallographic directions.

Table S3-2: Simulation parameters for individual experimental images

Acceleration voltage	300 kV
Defocus C_1	-2 nm
Spherical aberration constant C_3	10 μm
Specimen thickness	3 nm
Emitter energy spread	1 eV

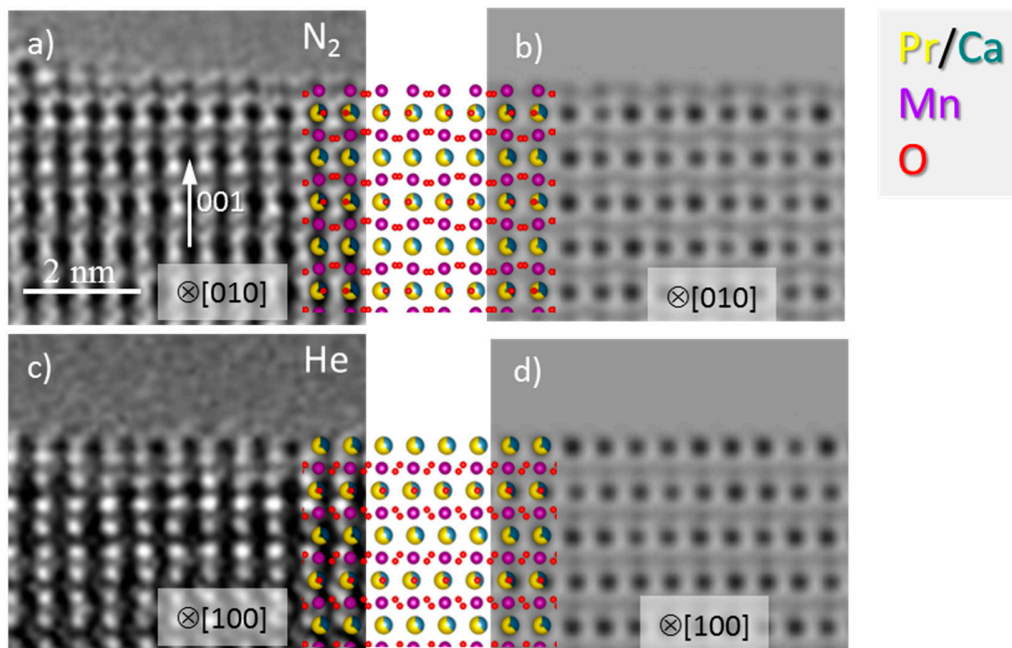


Figure S6-2. (a) Experimental HRTEM image and (b) corresponding calculated image of B-terminated surface of PCMO ($x=0.33$) projected along [010]. (c) Experimental HRTEM image and (d) corresponding calculated image of A-terminated surface of PCMO projected along [100]. The atomic models are shown in between.

The PCMO ($x=0.1$) after electron beam treatment in He at 50 μ bars.

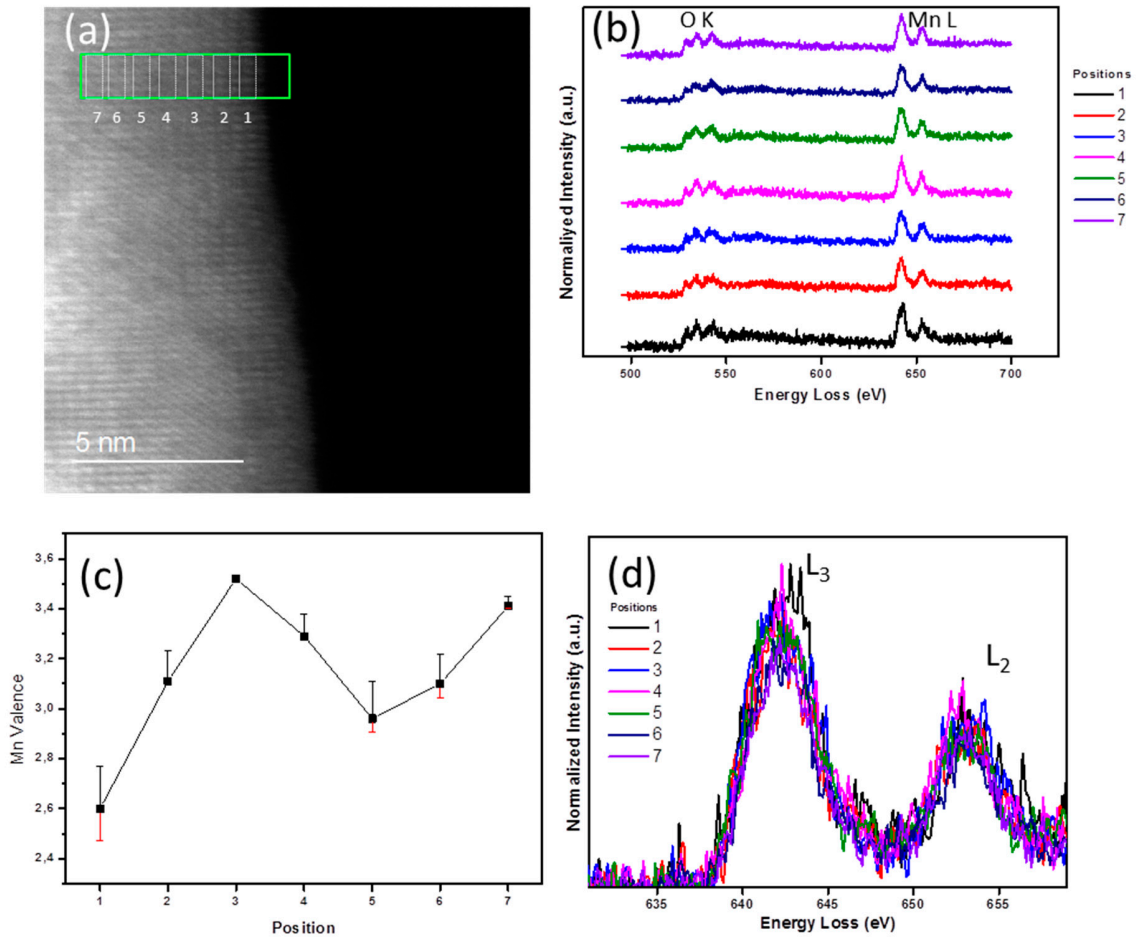


Figure S7. The PCMO ($x=0.1$) after electron beam treatment in He at 50 μ bars. (a) HAADF image; (b) EELS spectra; (c) Mn valence plot; (d) L_{2,3}-edge of Mn at each point.

Table S4. Summary of the Mn valence of PCMO ($x=0.1$) after electron beam treatment in He at 50 μ bars.

The average value is 3.14 ± 0.06

Position	1	2	3	4	5	6	7
Mn valence	2.6	3.11	3.52	3.29	2.96	3.10	3.41
Error (-)	-0.13	0	0	0	-0.054	-0.058	-0.01
Error (+)	0.17	0.12	0	0.09	0.15	0.12	0.04

Verification of structure and chemistry of particles formed at the amorphous edge.

The structure of nanoparticles formed at the amorphous edge of PCMO ($x=0.1; 0.33$) was identified using FFT analysis individually (Fig. S7) and by averaging over many particles similar to reported earlier (see Ref. 18 in the main text). The structure fits to the fcc cubic fluorite structure (Fm3m, $a=0.5393$ nm) of PrO_2 . Moreover, several particles were also analyzed using EELS. One of spectra is shown in Fig. S7b. Only O-K and Pr-M edges are present.

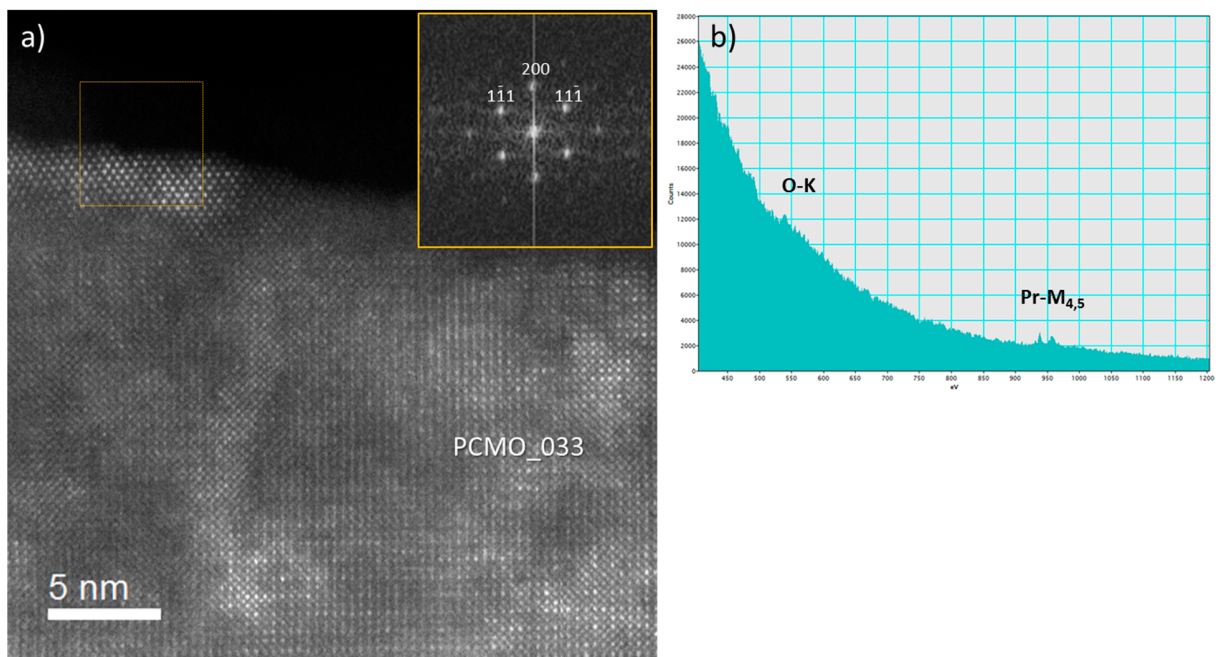


Figure S8. (a) HRSTEM image of PCMO ($x=0.33$) the corresponding FFTs is shown in the inset. (b) EELS spectrum taken from the particle shown in (a). The only O-K and Pr-M_{4,5} edges are present.

Control over the composition and purity of a gas before exposing the sample to the gas.

The mass spectrometry measurements with the rest gas analyzer (RGA) are controlled by the software program Quadera™.

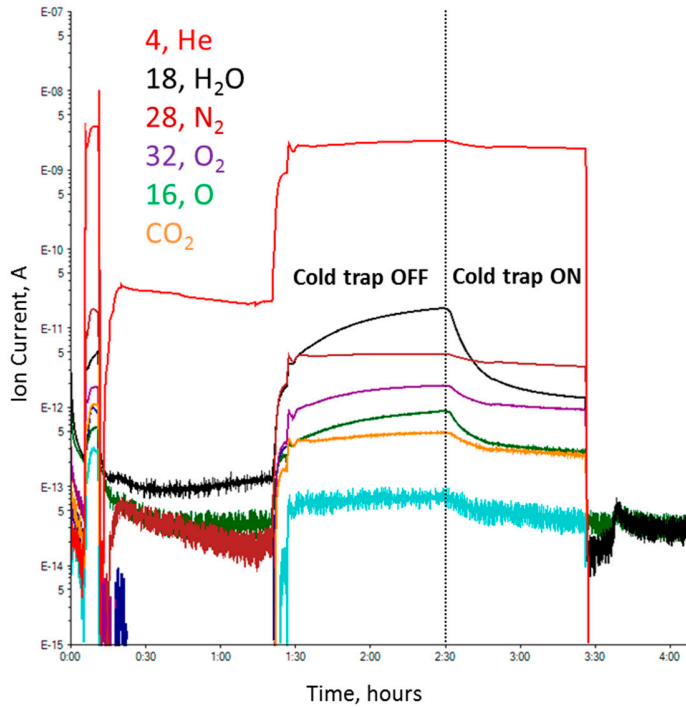


Figure S9 An example of multiple ion detection scan in Quadera™ for the experiment in He with and without using of cold trap.